International Journal of Solids and Structures 48 (2011) 2485–2495

Contents lists available at ScienceDirect

International Journal of Solids and Structures

journal homepage: www.elsevier.com/locate/ijsolstr

Buckling of delaminated bi-layer beam-columns

Fangliang Chen, Pizhong Qiao *

Department of Civil and Environmental Engineering, Washington State University, Sloan Hall 117, Pullman, WA 99164-2910, USA

ARTICLE INFO

Article history:
Received 15 February 2011
Received in revised form 18 April 2011
Available online 8 May 2011

Keywords:
Layered materials
Delamination
Debonding
Beam-columns
Composite beams
Buckling
Interface mechanics

ABSTRACT

An improved analytical model is presented to analyze the delamination buckling of a bi-layer beam-column with a through-the-width delamination. Both the transverse shear deformation and local delamination tip deformations are taken into consideration, and two delaminated sub-layers as well as two substrates in the intact (un-delaminated) regions are modeled as individual Timoshenko beams. A deformable interface is introduced to establish the continuity condition between the two substrates in the intact regions. Consequently, a flexible joint is formed at the delamination tip, and it is different from the conventional rigid joint given in most of studies in the literature, in which the local delamination tip deformations are completely ignored. In contrast to the local delamination buckling in our previous study (Qiao et al., 2010), the present model accounts for the global deformations of the intact region in the delaminated composite beam-column, thus capable of capturing the buckling mode shape transitions from the global, to global–local coexistent, and to local buckling for asymmetric delamination as the interface delamination increases. Good agreement of the present analytical solutions with the full 2-D elastic finite element analysis demonstrates the local deformation effects around the delamination tip and verifies the accuracy of the present model. Parametric studies are conducted to investigate the effects of loading eccentricity, delaminated sub-layer thickness ratio, and interface compliance on the critical buckling load for the delaminated composite beam-column. Transitions of buckling modes from the global to local delamination buckling are also disclosed as the thickness of one sub-layer reduces from the thick sub-layer to a thin film. The developed delamination buckling solution facilitates the design analysis and optimization of laminated composite structures, and it can be used with confidence in buckling analysis of delaminated composite structures.

1. Introduction

Due to manufacturing defects (e.g., imperfect curing process) or in-service accidents (e.g., low velocity impact), delamination may appear in laminated composite materials. Because of the presence of the delaminated area, the designed buckling strength of laminated structures can be reduced when subjected to compressive loading. Thus, as a major failure mode, the buckling of delaminated composite structures has been extensively studied in the literature.

Numerous studies have been attempted to model and analyze the buckling problem of delaminated beam- or plate-type composite structures. Including the bending-extension coupling, Chai et al. (1981) conducted one-dimensional buckling analysis of single delaminated composite laminate plates. Later, Chai (1982) developed one of the first analytical delamination models for homogeneous, isotropic plates using a thin-film model and extended this approach to a general bending case which includes the bending of a thick base laminate. Yin (1988) derived general formulae for thin-film strips with mid-plane symmetric delamination and evaluated the effects of laminated structures on delamination buckling and its growth. Based on the classical plate theory, Yin and his coworkers (Yin et al., 1986; Yin, 1998) conducted thermo-mechanical buckling and post-buckling analyses of multilayered laminates with an across-the-width delamination and presented the closed form solution of delamination buckling mode.

Due to low transverse shear modulus relative to the longitudinal Young's modulus in composite laminates, shear deformation was shown as a key factor influencing the delamination buckling behavior. Based on a variational energy approach, Chen (1991) proposed a shear deformation theory to study the delamination of one-dimensional (1-D) orthotropic homogeneous elastic beams. Considering large deflection of laminates, Chen (1993) later derived the closed form expressions for the critical buckling load and post-buckling deflection of asymmetric laminates. According to the studies (Chen, 1991, 1993), the inclusion of transverse shear deformation reduces the overestimation of buckling and ultimate load capacity of delaminated composite plates. In virtue of a perturbation technique, Kardomateas and Shmueser (1998) investigated the effect of transverse shear on buckling and post-buckling of a 1-D orthotropic elastic beam with a through-width

* Corresponding author. Tel.: +1 509 335 5183; fax: +1 509 335 7632.
E-mail address: qiao@wsu.edu (P. Qiao).

0020-7683/$ - see front matter © 2011 Elsevier Ltd. All rights reserved.
doi:10.1016/j.ijsolstr.2011.04.020

delamination. They found that the transverse shear effects prompt a reduction in the critical buckling load and an increase in the energy release rate.

When the delaminated beam-column is buckled, the potential interlayer slip exists between the intact substrates, leading to partial composite interaction and different longitudinal boundary conditions (Cas et al., 2007; Schnabl et al., 2007; Girhammar and Pan, 2007). Many analytical, numerical and experimental studies have been conducted in the literature to investigate the effect of this interlayer slip-induced partial composite interaction on the buckling behavior of delaminated beam-columns (Adam et al., 1997; Planinc et al., 2008; Kryzanowski et al., 2009; Battini et al., 2009; Schnabl and Planinc, 2010, 2011), and it was found that the developed interlayer slip in the delaminated layered structures has a significant effect on its critical buckling load. It should be mentioned that a linear bond slip constitutive law was often employed in most of the above mentioned studies to model the interlayer slip behavior. In reality, however, the interlayer slip between the delaminated sub-layers is a highly nonlinear failure behavior during slipping stage, which makes it unsuitable to attain the critical buckling load for a delaminated composite structure through eigenvalue-based analysis.

Because of the existence of delamination as well as the interface between the two substrates, elastic joints at delamination tips are formed, and a hybrid bi-layer composite beam-column with a through-the-width interface delamination can be divided into a total of six different sub-regions as shown in Fig. 1. However, most of existing studies in the literature (Moradi and Taheri, 1999; MSRao and Shu, 2004; Shu and MSRao, 2004; Kryzanowski et al., 2008) treated the intact region as a single composite beam. Consequently, the elastic deformations of the joint, such as differential axial extension and normal peeling of the two sub-layers are fully ignored, and the rotations of delaminated sub-layers and un-delaminated substrates around the delamination tips were artificially restricted to be identical, leading to a unrealistic rigid joint at the delamination tips, which is obviously contradictive with the real situation after the delaminated sub-layers buckle. It is well known that due to material mismatch of hybrid bi-layer beam-column, high stress concentration exists along the interface, especially at regions near the delamination tips, which makes the delamination tip deformations much more pronounced. As demonstrated in the studies (Qiao and Wang, 2004; Andrews and Massabo, 2007; Qiao and Chen, 2008, 2009, 2011; Wang and Zhang, 2009; Chen and Qiao, 2010), the delamination (crack) tip deformations play a crucial role affecting the interface stress distribution and energy release rate of delamination in layered structures. However, only few studies in the literature have taken the effect of delamination tip deformations into account while studying the buckling of delaminated composite structures. Recently, the authors (Qiao et al., 2010) investigated the effect of the delamination tip deformation on the sub-layer local delamination buckling in the bi-layer beams. The results revealed that with the inclusion of delamination tip deformations, the critical sub-layer local delamination buckling load decreases, and it is much closer to the numerical finite element results when compared with the overestimated delamination buckling load by the rigid joint model where the delamination tip deformations are fully neglected. However, the study in Qiao et al. (2010) neglected the global deformation of the intact sub-regions of the delaminated composite columns, which makes it only capable of predicting the sub-layer local delamination buckling under pure compression while fails to capture the global buckling of the whole bi-layer composite column. In most actual cases, however, the columns or beams are often under combined axial compression force and bending (e.g., via the eccentricity of axial compression force from the neutral axis), leading to composite laminated beam-columns.

To release the limitation in the previous study (Qiao et al., 2010) and improve the delamination buckling analysis of delaminated bi-layer beam-columns, the present model will account for both the global deformations of the intact substrates and local delamination tip deformations of the delaminated beam-columns. The objectives of this study are thus twofold: (1) to derive the closed-form analytical solution for the critical buckling load of an interface deformable delaminated composite beam-column with consideration of transverse shear, delamination tip deformation, and initial geometry imperfection (load eccentricity), and (2) to evaluate the effects of delaminated sub-layer thickness ratio, loading eccentricity, and delamination tip deformation on the critical buckling load.

2. Problem definition

Consider a delaminated bi-layer composite beam-column under general compression as shown in Fig. 1, where a delamination with a length of $2a$ lies along the interface of the top sub-layer "1" and bottom sub-layer "2" with thickness of h_1 and h_2, respectively. The two sub-layers in the composite beam-column span three regions of left intact, central delaminated, right intact portions with lengths of L_1, $2a$, and L_2, respectively, and they are made of homogenous, orthotropic materials, with the orthotropy axes along the coordinate system. The interface delamination is located at L_1 and L_2 from the left and right ends of the beam-column, respectively. It is assumed that (1) the lengths of the intact regions L_1 and L_2 are relatively large compared to the thickness of the whole composite beam so that the Saint–Venant's principle is satisfied, and (2) the lengths of delaminated and intact portions of the beam-column are relatively large compared to the sub-layer thickness so that a beam theory can be used to model the behavior of the top and bottom sub-layers.

To simplify the analysis, it is further assumed that a single symmetric interface delamination is present at the center of the composite beam-column (i.e., $L_1 = L_2$). Thus, only half of the specimen is modeled using a shear-release at the symmetric plane as shown in Fig. 2(a). It is assumed that the compression force P is applied at a distance e away from the neutral axis of the composite bi-layer beam-column (Fig. 2(b)). When $e = 0$, the considered beam-column is under pure compression. In this study, both the delaminated sub-layers and intact substrates are modeled as the layer-wise Timoshenko beams, and the flexible joint model (Qiao and Wang, 2004) is adopted to establish the continuity conditions among the delaminated and intact substrates at the delamination tip. As

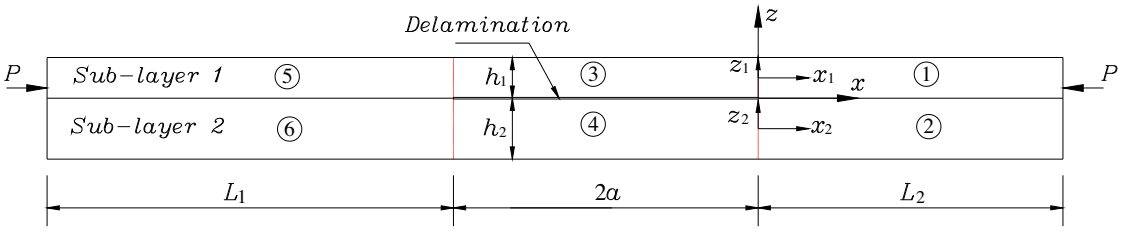

Fig. 1. A bi-layer composite beam-column with an interface delamination.

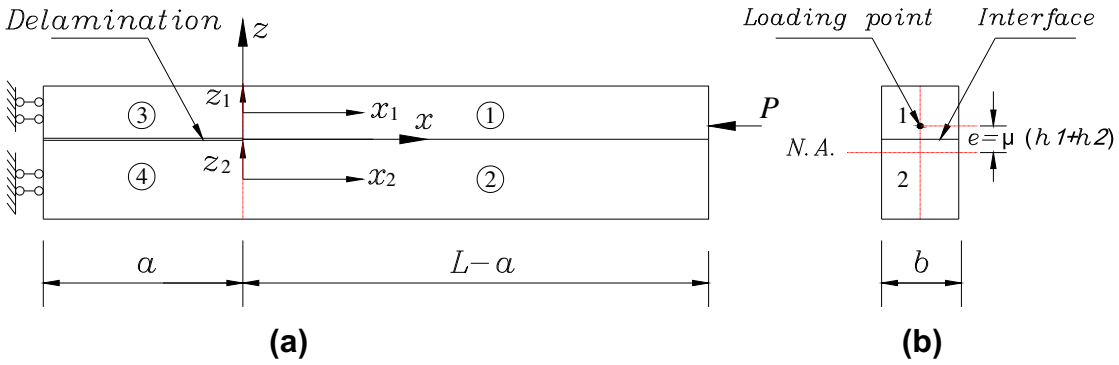

Fig. 2. A bi-layer composite beam-column with an interface delamination: (a) simplified symmetric model, and (b) beam cross section.

a result, the unrealistic restrictions in the rigid joint as stated previously is released and both the delaminated and intact sub-layers have their own individual deformations and rotations.

3. Buckling analysis by flexible joint model

As aforementioned, in most studies in the literature, the delamination tips are modeled as the rigid joints. However, as revealed by the recent study (Qiao et al., 2010), this kind of rigid joint model predicts an upper bound of the delamination buckling load. To release the rigid joint restrictions, the flexible joint model (Qiao and Wang, 2004) is introduced in this study to investigate the effect of the delamination tip deformations on buckling behavior of a delaminated bi-layer beam-column under general compression.

3.1. Flexible joint model and delamination tip deformations

For the convenience of buckling analysis of delaminated composite beam-columns, the flexible joint model (Qiao and Wang, 2004) is briefly introduced. The deformation field at delamination tip is emphasized, and it is later used to derive the solution for the buckling load of the delaminated composite beam-column.

A typical infinitesimal isolated body of the bi-layer beam is shown in Fig. 3(a), and the following equilibrium equations are established:

$$\frac{dN_1(x)}{dx} = b\tau(x), \quad \frac{dN_2(x)}{dx} = -b\tau(x), \tag{1a}$$

$$\frac{dQ_1(x)}{dx} = b\sigma(x), \quad \frac{dQ_2(x)}{dx} = -b\sigma(x), \tag{1b}$$

$$\frac{dM_1(x)}{dx} = Q_1(x) - b\tau(x)\frac{h_1}{2}, \quad \frac{dM_2(x)}{dx} = Q_2(x) - b\tau(x)\frac{h_2}{2}, \tag{1c}$$

$$N_1(x) + N_2(x) = N_{10} + N_{20} = N_T(x), \tag{1d}$$

$$Q_1(x) + Q_2(x) = Q_{10} + Q_{20} = Q_T(x), \tag{1e}$$

$$M_1(x) + M_2(x) + N_1(x)\frac{h_1 + h_2}{2} = M_{10} + M_{20} + N_{10}\frac{h_1 + h_2}{2} + Q_T(x) = M_T(x), \tag{1f}$$

where $N_i(x)$, $Q_i(x)$, and $M_i(x)$ are the internal axial forces, transverse shear forces, and bending moments in the intact substrates i ($i = 1, 2$), respectively; N_{i0}, Q_{i0}, and M_{i0} are the axial, transverse shear forces, and bending moments in the delaminated sub-layers j ($j = 3, 4$), N_T, Q_T, and M_T are the total applied axial and transverse shear forces and bending moment, respectively, expressed by the right equality (see Fig. 3(a)). For convenience, it is defined that all the resulting applied forces act on the neutral axis of sub-layer 2. In this way, M_2 only relates to N_1 and M_1; b is the width of composite beam. h_1 and h_2 are the thickness of sub-layers 1 and 2, respectively; $\sigma(x)$ and $\tau(x)$ are the interface normal and shear stresses, respectively.

According to Timoshenko beam theory, the forces and displacements of each sub-layer can be related as:

$$N_i(x) = A_i\frac{du_i(x)}{dx}, \tag{2a}$$

$$M_i(x) = D_i\frac{d\phi_i(x)}{dx}, \tag{2b}$$

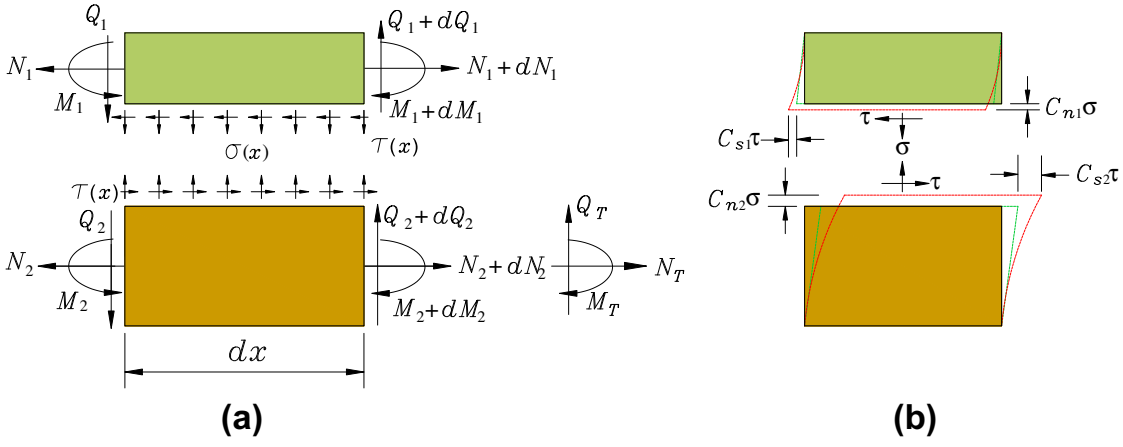

Fig. 3. Configuration of a bi-layer beam: (a) infinitesimal isolated body, and (b) displacement continuity along the interface in flexible joint model.

$$Q_i(x) = B_i\left(\frac{dw_i}{dx} + \phi_i\right), \tag{2c}$$

where $u_i(x)$, $w_i(x)$ and $\phi_i(x)$ are the longitudinal displacement, transverse displacement, and rotation of sub-layers i ($i = 1, 2$), respectively; A_i, B_i, and D_i are the axial, transverse shear and bending stiffness of beams i ($i = 1, 2$), respectively, and $A_i = E_i b h_i$, $B_i = 5G_i b h_i/6$, and $D_i = E_i I_i$ (where E_i, G_i and I_i are the Young's modulus, transverse shear modulus, and the moment of inertia of sub-layer i ($i = 1, 2$), respectively).

In the flexible joint model, the deformation induced by the interface stresses along the interface is accounted for by introducing two interface compliance coefficients. As a result, the differential displacements and rotation of each substrate at the delamination tip are allowed (see Fig. 4(c)), which is closer to the real deformation state of the buckled delaminated bi-layer beam-column in contrast to the unrealistic rigid restriction of the deformation state in the conventional rigid joint model (see Fig. 4(a)). The continuity conditions of deformation along the interface are expressed as (Fig. 3(b))

$$w_1(x) - C_{n1}\sigma(x) = w_2(x) + C_{n2}\sigma(x), \tag{3}$$

$$u_1(x) - \frac{h_1}{2}\phi_1(x) - C_{s1}\tau(x) = u_2(x) + \frac{h_2}{2}\phi_2(x) + C_{s2}\tau(x), \tag{4}$$

where C_{ni} and C_{si} are the interface compliance coefficients of sub-layer i under the interface normal and shear stresses, respectively, and they account for the contribution of interface stresses to the displacement components at the bonded interface. Estimations of these two interface compliances (Wang and Qiao, 2004a) are given as follows:

$$C_{si} = \frac{h_i}{15G_{13}^{(i)}}, \quad C_{ni} = \frac{h_i}{10E_{33}^{(i)}}, \tag{5}$$

where $E_{33}^{(i)}, G_{13}^{(i)} (i = 1, 2)$ are the through-thickness Young's modulus and transverse shear modulus of sub-layer i, respectively. It is noted that the shear deformable bi-layer beam theory (Wang and Qiao, 2004b) can be retrieved by ignoring the two interface compliance coefficients (i.e., $C_{ni} = C_{si} = 0$), leading to a "semi-rigid" joint at the delamination tip. In this case, only the partial delamination tip deformation (i.e., the differential rotations of delaminated sub-layers and un-delaminated substrates) is accounted for (see Fig. 4(b)).

Combining the equilibrium equations (Eq. (1)), the constitutive equations (Eq. (2)), and the continuity equations (Eqs. (3) and (4)), the governing equation of the intact bi-layer beam system can be established as

$$a_6\frac{d^6N_1}{dx^6} + a_4\frac{d^4N_1}{dx^4} + a_2\frac{d^2N_1}{dx^2} + a_0N_1 + a_MM_T + a_NN_T = 0, \tag{6}$$

where

$$a_6 = \frac{1}{b^2K_nK_s}, \quad a_4 = -\left(\eta + \frac{h_1}{2}\xi\right)\frac{1}{bK_n} - \left(\frac{1}{B_1} + \frac{1}{B_2}\right)\frac{1}{bK_s},$$

$$a_2 = \left(\frac{1}{B_1} + \frac{1}{B_2}\right)\left(\frac{\eta}{\xi} + \frac{h_1}{2}\right) + \left(\frac{1}{D_1} + \frac{1}{D_2}\right)\frac{1}{bK_s},$$

$$a_0 = -\left(\frac{1}{D_1} + \frac{1}{D_2}\right)\eta - \frac{(h_1 + h_2)}{2D_2}\xi$$

$$a_M = \left(\frac{1}{D_1} + \frac{1}{D_2}\right)\frac{h_2}{2D_2} + \frac{\xi}{D_2}, \quad a_N = \frac{1}{A_2}\left(\frac{1}{D_1} + \frac{1}{D_2}\right)$$

and $K_n = C_{n1} + C_{n2}$, $K_s = C_{s1} + C_{s2}$; $\xi = \frac{h_1}{2D_1} - \frac{h_2}{2D_2}$, $\eta = \frac{1}{A_1} + \frac{1}{A_2} + \frac{h_2(h_1+h_2)}{4D_2}$.

The resultant forces and bending moments of each substrate can be obtained by using the characteristic equation of Eq. (6) with roots as: (a) $\pm R_1$, $\pm R_2$, and $\pm R_3$, or (b) $\pm R_1$ and $\pm R_2 \pm iR_3$. Here, R_1, R_2, and R_3 are three real numbers. For brevity, only the resultant forces of two sub-layers in Case (a) is given as follows for instance (the other case can be referred to – Qiao and Wang (2004)).

$$N_1(x) = \sum_{i=1}^{3} c_ie^{-R_ix} + N_{1C},\ M_1(x) = \sum_{i=1}^{3} c_iS_ie^{-R_ix} + M_{1C},\ Q_1(x) = \sum_{i=1}^{3} c_iT_ie^{-R_ix} + Q_{1C} \tag{7a}$$

$$N_2(x) = -\sum_{i=1}^{3} c_ie^{-R_ix} + N_{2C},\ M_2(x) = -\sum_{i=1}^{3} c_iS_i'e^{-R_ix} + M_{2C},$$

$$Q_2(x) = -\sum_{i=1}^{3} c_iT_ie^{-R_ix} + Q_{2C} \tag{7b}$$

where the coefficients in Eq. (7) are given in the Appendix; $N_{iC}(x)$, $Q_{iC}(x)$, and $M_{iC}(x)$, are the internal forces of substrates i ($i = 1, 2$) based on the conventional composite beam theory (rigid joint model), which can be expressed as

$$N_{1C} = -\frac{a_M}{a_0}M_T - \frac{a_N}{a_0}N_T, \quad N_{2C} = N_T - N_{1C}, \tag{8a}$$

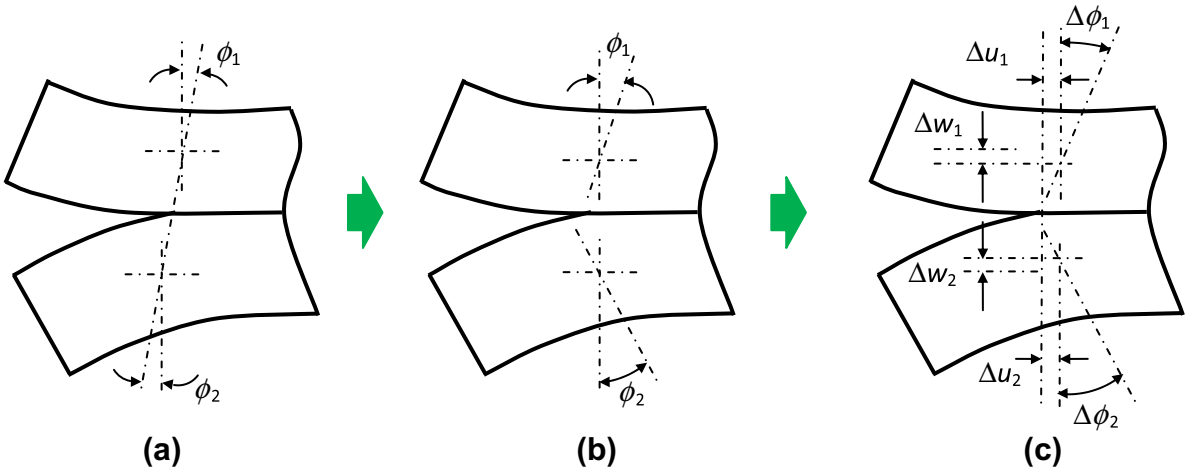

Fig. 4. Delamination tip deformations in different joint models: (a) the conventional rigid joint; (b) the semi-rigid joint; and (c) the flexible joint.

$$M_{1C} = -\left(\frac{\eta}{\xi}\frac{a_M}{a_0} + \frac{h_2}{2D_2\xi}\right)M_T - \left(\frac{\eta}{\xi}\frac{a_N}{a_0} + \frac{1}{A_2\xi}\right)N_T,$$

$$M_{2C} = M_T - M_{1C} - \frac{h_1+h_2}{2}N_{1C}, \tag{8b}$$

$$Q_{1C} = -\left(\left(\frac{\eta}{\xi} + \frac{h_1}{2}\right)\frac{a_M}{a_0} + \frac{h_2}{2D_2\xi}\right)Q_T, \quad Q_{2C} = Q_T - Q_{1C}. \tag{8c}$$

The interface stresses are then obtained as:

$$\sigma(x) = \frac{dQ_1(x)}{bdx} = -\frac{1}{b}\sum_{i=1}^{3} c_i R_i T_i e^{-R_i x} + \sigma_C, \tag{9a}$$

$$\tau(x) = \frac{dN_1(x)}{bdx} = -\frac{1}{b}\sum_{i=1}^{3} c_i R_i e^{-R_i x} + \tau_C, \tag{9b}$$

where

$$\tau_C = \frac{dN_{1C}}{bdx}, \quad \sigma_C = \frac{dQ_{1C}}{bdx}. \tag{10}$$

The local deformations of the delamination tip can finally be established as

$$\begin{Bmatrix} \Delta u_1^F(0) \\ \Delta u_2^F(0) \\ \Delta\phi_1^F(0) \\ \Delta\phi_2^F(0) \\ \Delta w_1^F(0) \\ \Delta w_2^F(0) \end{Bmatrix} = \begin{pmatrix} u_1^F(0) \\ u_2^F(0) \\ \phi_1^F(0) \\ \phi_2^F(0) \\ w_1^F(0) \\ w_2^F(0) \end{pmatrix} - \begin{pmatrix} u_1^R(0) \\ u_2^R(0) \\ \phi_1^R(0) \\ \phi_2^R(0) \\ w_1^R(0) \\ w_2^R(0) \end{pmatrix} = \begin{pmatrix} S_{11} & S_{12} & S_{13} \\ S_{21} & S_{22} & S_{23} \\ S_{31} & S_{32} & S_{33} \\ S_{41} & S_{42} & S_{43} \\ S_{51} & S_{52} & S_{53} \\ S_{61} & S_{62} & S_{63} \end{pmatrix} \begin{pmatrix} N \\ M \\ Q \end{pmatrix}, \tag{11}$$

where $S = \{S_{ij}\}_{6\times 3}$ is a matrix representing the local deformation compliance at the delamination tip and given in Appendix. $\{u_1^F(0),\ u_2^F(0),\ \phi_1^F(0),\ \phi_2^F(0),\ w_1^F(0),\ w_2^F(0)\}^T$ represents the displacement components of the respective intact substrates at the delamination tip by the flexible joint model; $\{u_1^R(0),\ u_2^R(0),\ \phi_1^R(0),\ \phi_2^R(0),\ w_1^R(0),\ w_2^R(0)\}^T$ represents the displacement components at the delamination tip based on the conventional rigid joint model. The superscripts "*F*" and "*R*" are used to denote the solutions based on the flexible and rigid joint models, respectively. $\{\Delta u_1^F(0),\ \Delta u_2^F(0),\ \Delta\phi_1^F(0),\ \Delta\phi_2^F(0),\ \Delta w_1^F(0),\ \Delta w_2^F(0)\}^T$ is the delamination tip deformations and expressed as the difference between the rigid and flexible joint models. *N*, *M*, *Q* are a group of self-equilibrium loading parameters acting at the delamination tip, which are defined as

$$N = N_{1C}(0) - N_{10}, \tag{12a}$$

$$Q = Q_{1C}(0) - Q_{10}, \tag{12b}$$

$$M = M_{1C}(0) - M_{10}. \tag{12c}$$

3.2. Governing equations of delaminated beam-columns

For a laminated composite beam-column, the shear deformation can be taken into account in a generalization of Timoshenko beam theory. The governing differential equations for the delaminated beam-column with constant cross sections under constant compression can be expressed as (Bažant and Cedolin, 1991):

$$D_j\frac{d^3\phi_j}{dx^3} + P_j\frac{d^2w_j}{dx^2} = p, \quad (j = 1 \text{ to } 4), \tag{13a}$$

$$D_j\frac{d^2\phi_j}{dx^2} + B_j\left(\frac{dw_j}{dx} - \phi_j\right) = 0, \quad (j = 1 \text{ to } 4), \tag{13b}$$

where $\phi_j(x)$ and $w_j(x)$ are the rotations and transverse displacements of beam regions j (j = 1–4) (Fig. 2(a)), respectively; $P_j = -N_j$ is the resultant compressive force applied at the neutral axis of sub-layers j (j = 1–4), and p is the transverse distributed load; B_j and D_j are the transverse shear and bending stiffness, respectively, and $B_j = 5G_jbh_j/6$ and $D_j = E_jI_j$ (G_j, E_j and I_j are the transverse shear modulus, Young's modulus and the moment of inertia of beam regions j (j = 1–4) in Fig. 2(a), respectively; b is the width of the composite beam-column).

When $p = 0$, the general solution of Eq. (13) can be obtained as (Bažant and Cedolin, 1991):

$$w_j(x) = C_1^j + C_2^j\cos k_j x + C_3^j x + C_4^j \sin k_j x, \quad (j = 1 \text{ to } 4), \tag{14a}$$

$$\phi_j(x) = -\beta_j C_2^j k_j \sin k_j x + C_3^j + \beta_j C_4^j k_j \cos k_j x, \quad (j = 1 \text{ to } 4), \tag{14b}$$

where $k_j^2 = \frac{P_j/D_j}{1-P_j/B_j}$ and $\beta_j = 1 - P_j/B_j$.

Due to the symmetry of the delamination area in the beam with respect to the center line (see Fig. 2(a)), the rotations and transverse displacements of the delaminated sub-layers can be reduced as

$$w_j(x) = C_1^j + C_2^j\cos k_j x, \quad (j = 3, 4), \tag{15a}$$

$$\phi_j(x) = -\beta_j C_2^j k_j \sin k_j x, \quad (j = 3, 4). \tag{15b}$$

3.3. Boundary and continuity conditions

It is assumed that the considered specimen is simply supported at both ends, and the boundary conditions for different regions and the continuity conditions for the considered problem in Fig. 2(a) can be expressed as

At $x = L - a$:

$$w_j = 0, \quad (j = 1, 2), \tag{16a}$$

$$\phi_{j,x} = 0, \quad (j = 1, 2), \tag{16b}$$

At $x = -a$:

$$\phi_j = 0, \quad (j = 3, 4). \tag{17}$$

The continuity conditions at the delamination tip (Fig. 2(a)) are:

At $x = 0$:

$$w_1 = w_3, \quad w_2 = w_4, \tag{18a}$$

$$\phi_1 = \phi_3, \quad \phi_2 = \phi_4, \tag{18b}$$

$$w_1 + \Delta w_1^F = w_2 + \Delta w_2^F, \tag{18c}$$

$$\phi_1 + \Delta\phi_1^F = \phi_2 + \Delta\phi_2^F, \tag{18d}$$

where Δw_j^F and $\Delta\phi_j^F$ are the local deformation of the delamination tip as defined in Eq. (11). It can be seen from Eq. (18) that the continuity conditions considered in this study allow the delaminated sub-layers and intact composite substrates at the location of the delamination tip have their respective deformations, and as a result, a flexible joint is formed at the delamination tip, with which the local delamination tip deformation are taken into account, which is thus different from the conventional rigid joint as shown in most existing studies in the literature where both the rotation and deformations of each sub-sections are artificially restrained to be identical. As already demonstrated in the sub-layer local delamination buckling (Qiao et al., 2010), an equivalent but relatively longer effective length ratio of the local delamination buckling is achieved by considering the local delamination tip deformation.

A set of equations thus consist of six boundary conditions (Eqs. (16) and (17)) and six continuity conditions (Eq. (18)), leading to a total of 12 equations for 12 unknown coefficients, i.e., C_1^j, C_2^j, C_3^j

and C_4^j (j = 1,2), C_1^j and C_2^j ($j = 3, 4$). These equations are linear and homogenous, and the coefficients of 12 unknowns can be written in a matrix. The equations are constructed in the following matrix form:

$$\mathbf{k}\boldsymbol{\alpha} = 0, \tag{19}$$

where $\mathbf{K}$ denotes the 12×12 matrix of coefficients, and α is the vector of 12 unknowns. Only the nontrivial solutions are of interest, where all the unknown parameters are not equal to zero. For a nontrivial solution, where $\boldsymbol{\alpha} \neq \mathbf{0}$, the lowest value of load P is sought, such that the determinant of the coefficient matrix $\mathbf{K}$ must vanish and the lowest value gives the critical buckling load. However, due to the complexity of the delamination tip deformation considered in this study, the analytical expressions for det($\mathbf{K}$) are too complicated to be presented as explicit closed-form formulas.

4. Comparisons and validation

The validity of the proposed method will be demonstrated in this section by comparing the present analytical solution with the ones predicted by the conventional rigid joint model, the semi-rigid joint model, and finite element analysis (FEA). In the comparison, the solutions based on the rigid joint model can be easily obtained by neglecting the delamination tip deformations, i.e., setting the delamination tip deformations in the continuity equations of Eq. (18) to be zero, while the semi-rigid joint model are reduced from the flexible joint model by simply neglecting the interface deformations, i.e., setting the interface compliances C_{ni} and C_{si} in Eq. (5) to be zero. The finite element (FE) results are taken as benchmark in the present numerical comparisons. In FEA, there are two major steps. The first one is to determine the stresses under the given boundary conditions and loading system through a linear static analysis; while the second one is to obtain the results in terms of load factors (eigenvalues) and buckling mode shapes (eigenvectors) through an eigenvalue analysis. In the FE modeling, the delaminated bi-layer beam-column is modeled by the commercial finite element package ANSYS10.0 as a plane stress structural plane element (PLANE42). To better capture the local deformations near the delamination tips and preserve more accurate numerical results, the refined elements at locations near the delamination tips are employed. The finite element arrangement and a typical buckled mode shape of the delaminated bi-layer beam-column are shown in Fig. 5.

A composite bi-layer beam-column specimen with interface delamination under pure end-loaded compressions (e = 0) is first examined. The composite beam with both isotropic ($E^{(1)} = E^{(2)} =$ 100 GPa, $\upsilon^{(1)} = \upsilon^{(2)} = 0.3$) and orthotropic ($E_{11}^{(1)} = E_{11}^{(2)} = 100$ GPa, $E_{33}^{(1)} = E_{33}^{(2)} = 10$ GPa, $G_{13}^{(1)} = G_{13}^{(2)} = 5$ GPa, $\upsilon_{13}^{(1)} = \upsilon_{13}^{(2)} = 0.3$) material properties are analyzed. In the following analysis, the obtained critical buckling load (P_{cr}) is normalized with respect to the classical Euler buckling load (P_E) of the intact composite beam in order to present the buckling behavior and manifest the influence of various parameters, i.e.,

$$\overline{P}_{cr} = \frac{P_{cr}}{P_E} = \frac{P_{cr}}{4\pi^2 D_{11}/L^2}, \tag{20}$$

where D_{11} is the bending stiffness of the intact composite beam-column.

Comparisons of normalized buckling loads with respect to different delamination length ratios (a/L) among different joint models and FEA are shown in Figs. 6 and 7 for a simply supported bi-layer beam-column (without any eccentricity) with isotropic and orthotropic material properties, respectively. To better compare the predictions by different models, the solutions are also listed in Tables 1 and 2, where some available solutions in the literature based on the assumption of rigid joint at the delamination tips are also compared (Parlapalli and Shu, 2004; Kryzanowski et al., 2008). The slenderness ratios of the bi-layer beam-column, $L/(h_1 + h_2)$, for both the materials are fixed to be 5, and the total thickness of the composite bi-layer column is unit. The symmetric delamination buckling (where $h_1/(h_1 + h_2) = 0.5$ and each sub-layer has the same geometry and material properties) and asymmetric delamination buckling (where $h_1/(h_1 + h_2) = 0.1$, and each sub-layer has the same material properties) are, respectively, analyzed. In Figs. 6 and 7, as expected, the normalized buckling load decreases with the increasing of the delamination length ratio for both symmetric and asymmetric delamination buckling. It can be further found that the normalized buckling load in the asymmetric delamination case (Figs. 6(b) and 7(b)) reduces much more rapidly after the delamination length ratio grows larger than 0.2; among different models, as the delamination grows to a relatively large level (e.g., a/L approaches to 1.0), all the solutions asymptotically converge to the same one, indicating the reduced effects of local delamination tip deformation and transverse shear. As shown in Fig. 6(b), for the asymmetric delamination buckling, the buckling mode shape of the bi-layer beam-column changes with the increasing of the delamination length ratio. When the delamination length or the slenderness ratio of the delaminated sub-layer is relatively small (e.g., $a/L < 0.2$, or $a/h_1 < 10$), the whole beam-column is globally buckled, indicating that the critical buckling load is primarily controlled by the global buckling (Euler buckling) behavior. When the delamination length or the slenderness ratio of the delaminated sub-layer is relatively large (e.g., $a/L > 0.4$ or $a/h_1 > 20$), only the thin delaminated sub-layer is buckled, implying that the critical buckling load of the bi-layer beam-column is dominantly controlled by the local delamination buckling of the thin sub-layer. Between these two slenderness ratios, i.e., when $0.2 < a/L < 0.4$, or $10 < a/h_1 < 20$, the global buckling of the whole beam and the local

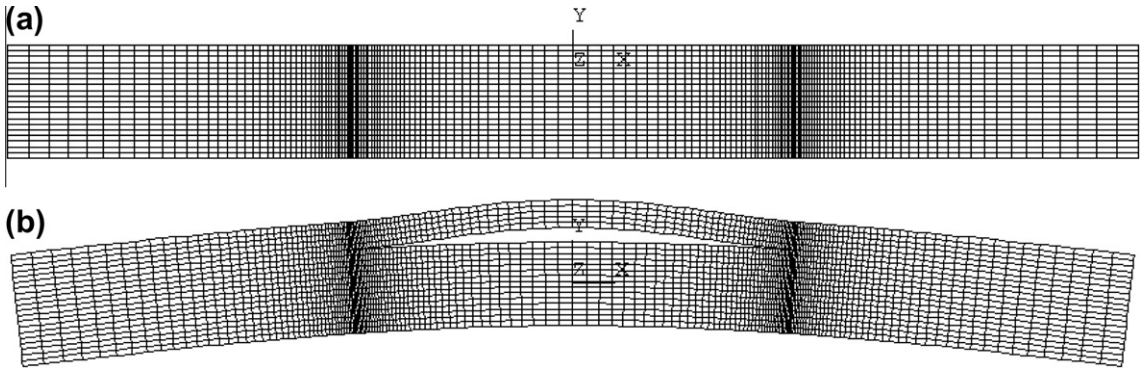

Fig. 5. FE model of the bi-layer beam-column with through-the-width delamination: (a) mesh of the whole specimen; and (b) a typical buckling mode shape.

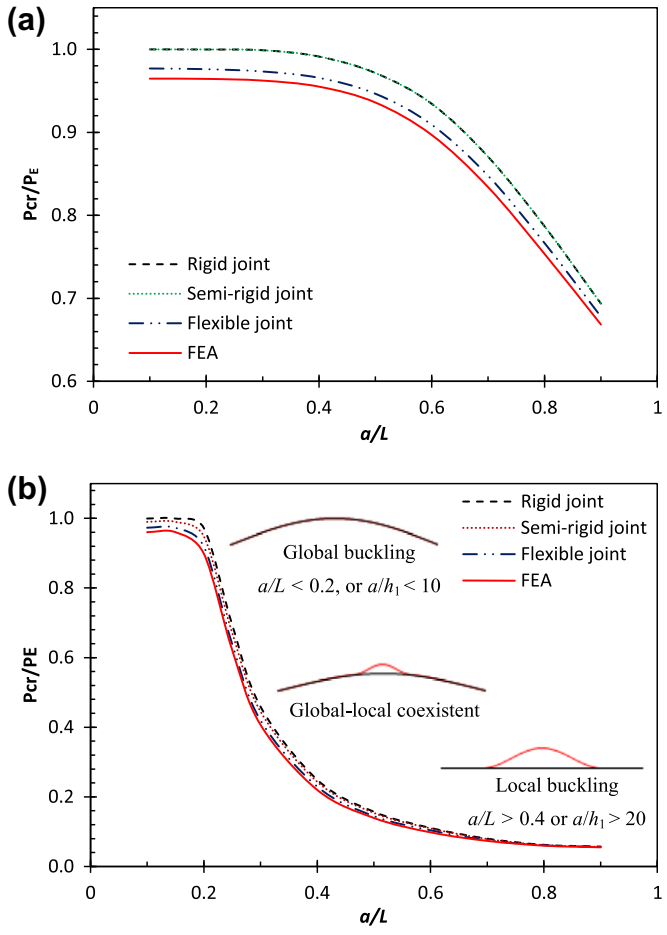

Fig. 6. Comparisons of normalized buckling load among different models for isotropic bi-layer beam-column: (a) symmetric delamination buckling, and (b) asymmetric delamination buckling.

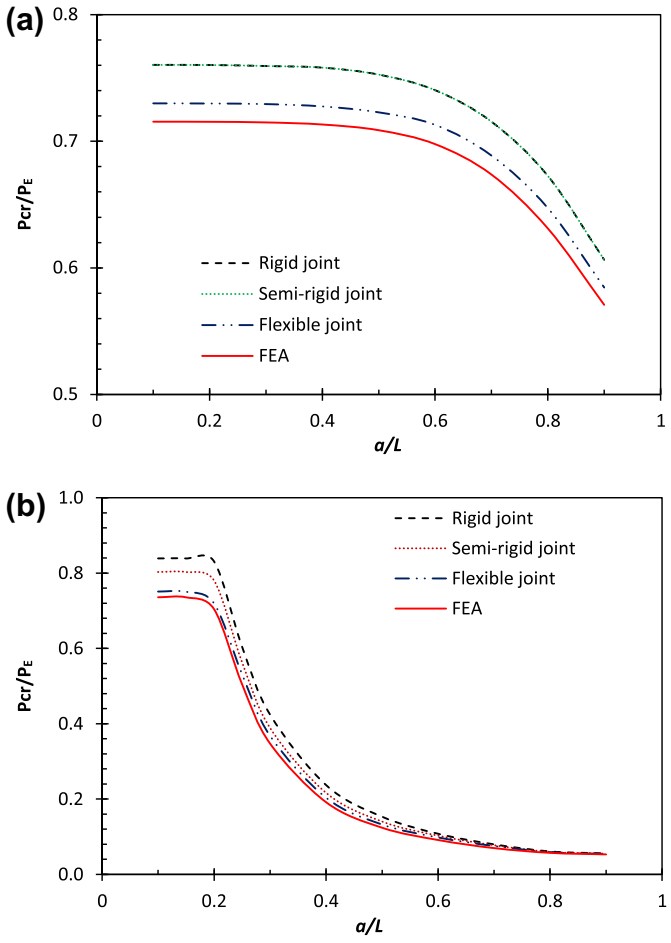

Fig. 7. Comparisons of normalized buckling load among different models for orthotropic bi-layer beam-column: (a) symmetric delamination buckling, and (b) asymmetric delamination buckling.

buckling of the delaminated sub-layer co-exist. It should be mentioned that there is no unique definition of buckling modes for delaminated beam-columns in the literature. According to the study (Short et al., 2001), the categorization of buckling modes was primarily based on the delamination geometry, where the local mode occurs when the upper sub-laminate is thin and the area of delamination is large; and the global mode is observed when the delamination has a small area and is deeper through the thickness. While in the studies of Kryzanowski et al. (2008) and Ovesy and Kharazi (2011), the buckling modes were characterized by the buckling mode shapes. Thus, the classification of the buckling modes in this study follows those classifications (Kryzanowski et al., 2008; Ovesy and Kharazi, 2011), i.e., different buckling modes are classified from the apparent mode shapes rather than any theoretically definitions.

As shown in Fig. 6(a), the solutions predicted by the semi-rigid joint model are identical with those provided by the rigid joint model, indicating that the semi-rigid joint model cannot provide better predication of critical buckling load for the symmetric delamination buckling than the conventional rigid joint model. This phenomenon is due to the fact that the semi-rigid joint model only releases the restraint on the rotation of both the sub-layers at the delamination tip, which has no effect on the solution when the specimen consisting of two symmetric sub-layers under pure compression or bending moment. The rotations of the two sub-layers in this symmetric delamination case are in fact identical. While for the asymmetric delamination buckling, there exists different rotation of each sub-layer after it buckles. Due to the release of the restriction on the rotation of each sub-layer, the semi-rigid joint model is able to capture the local rotation effect of sub-layers at the delamination tip, and it thus provides better predications of the critical buckling loads than the rigid joint model (see Figs. 6(b) and 7(b)). Nevertheless, because the deformation at the delamination tip is fully restrained in the rigid joint model and only the individual sub-layer rotations are allowed while individual displacements are prohibited in the semi-rigid joint model, both these two models overestimated the critical buckling load compared with the FEA. Through releasing the local delamination tip deformation such that each sub-layer has their individual rotation and elastic deformation at the delamination tip, the local delamination tip deformation is retrieved by the flexible joint model. As a result, the critical buckling loads predicted by the flexible joint model are much closer to those evaluated by FEA (see Figs. 6 and 7), which verifies the accuracy and improvement offered by the present solution. On the other hand, it manifests that the local delamination tip deformation plays an important role in accurately evaluating the critical buckling load, especially for the material with the low transverse shear modulus (i.e., orthotropic vs. isotropic materials) and when the delamination ratio (a/L) is small.

5. Parametric studies

To further illustrate the improved accuracy brought by the present solution and shed light on the effects of local delamination tip

Table 1
Normalized buckling load for simply supported bi-layer beam-columns with isotropic material property.

a/L	$h_1/(h_1+h_2)=0.1$				$h_1/(h_1+h_2)=0.5$			
	0.2	0.4	0.6	0.8	0.2	0.4	0.6	0.8
Rigid joint model	0.9723	0.2494	0.1109	0.0624	0.9997	0.9912	0.9343	0.7867
MSRao and Shu (2004)	0.9723	0.2494	0.1109	0.0624	0.9997	0.9912	0.9343	0.7867
Kryzanowski et al. (2008)	0.9723	0.2494	0.1109	0.0624	0.9997	0.9912	0.9343	0.7867
Semi-rigid joint model	0.9487	0.2431	0.1093	0.0613	0.9997	0.9912	0.9343	0.7867
Flexible joint model	0.9193	0.2295	0.1038	0.0607	0.9759	0.9655	0.9090	0.7660
FEA	0.8985	0.2197	0.0976	0.0594	0.9643	0.9550	0.8967	0.7534

Table 2
Normalized buckling load for simply supported bi-layer beam-columns with orthotropic material property.

a/L	$h_1/(h_1+h_2)=0.1$				$h_1/(h_1+h_2)=0.5$			
	0.2	0.4	0.6	0.8	0.2	0.4	0.6	0.8
Rigid joint model	0.8307	0.2374	0.1082	0.0613	0.7602	0.7581	0.7403	0.6726
Semi-rigid joint model	0.7801	0.2165	0.1027	0.0598	0.7602	0.7581	0.7403	0.6726
Flexible joint model	0.7194	0.2038	0.0983	0.0594	0.7297	0.7274	0.7129	0.6472
FEA	0.7099	0.2199	0.1055	0.0665	0.7153	0.7132	0.6977	0.6312

deformations and transverse shear on the critical buckling load of the delaminated composite beam-column, a parametric study is conducted in this section. The critical buckling load of a delaminated beam-column depends on various loading, geometric and material parameters. In this section, the influences of a few key factors (e.g., delaminated sub-layer thickness ratio, loading eccentricity, and interface compliance) on the buckling load are analyzed.

5.1. Effect of delaminated sub-layer thickness ratio

The variations of the normalized critical buckling load with respect to the delaminated sub-layer thickness ratio $h_1/(h_1+h_2)$ for three different delamination length levels ($a/L=0.2$, $a/L=0.4$, and $a/L=0.6$) are compared and shown in Fig. 8. The loading, geometry and material properties of the bi-layer beam-column are the same as the isotropic case examined in Section 4. In this examination, the delaminated sub-layer thickness ratio $h_1/(h_1+h_2)$ varies from 0.05 (thin film delamination buckling) to 0.5 (symmetric delamination buckling). It can be seen from Fig. 8 that when the delamination length ratio is relatively small (e.g., $a/L \leqslant 0.2$), the change of the delaminated sub-layer thickness does not affect the normalized critical buckling load much, which implies that the buckling strength is relatively independent of the through-thickness position of the delamination for a short delamination. With the growth of the delamination (i.e., the increase of a/L), the normalized buckling load reduces rapidly with the decrease of the delaminated sub-layer thickness ratio, indicating that, as the delamination moves outward the surface from the mid-plane, the loading capacity of the beam-column will rapidly decrease. Fig. 9 shows the buckling mode shapes of the same beam-column (without any loading eccentricity) with a fixed delamination length ratio of $a/L=0.4$ for different delaminated sub-layer thickness ratios. It indicates that the buckling mode shape changes from the global buckling, to global-local coexistent buckling, and to local sub-layer delamination buckling as the position of delamination gradually moves from inside to outside of the beam-column or the thickness of one sub-layer decreases. As shown in Fig. 9, when there is a thin delaminated sub-layer (thin debonded film), the critical buckling load of the beam-column is more controlled by the local delamination buckling of the thin sub-layer, resulting in a significantly lower buckling strength when compared to the Euler buckling load of the intact beam-column.

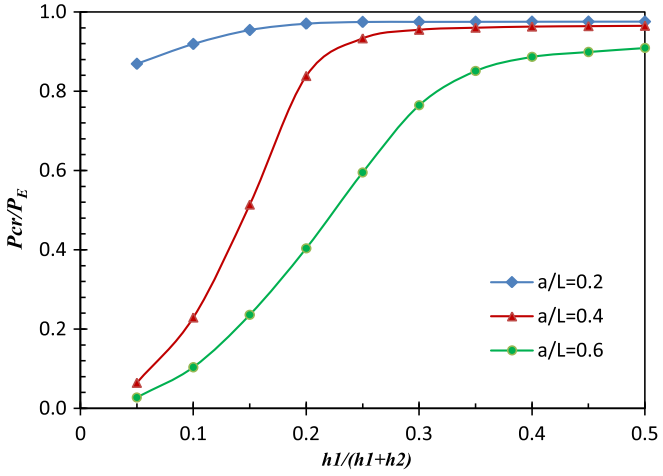

Fig. 8. Effect of delaminated sub-layer thickness ratio on the normalized critical delamination buckling load in bi-layer beam-column.

5.2. Effect of loading eccentricity

To examine the initial imperfection of the beam-column such as initial curve of the structure or loading eccentricity, the effect of the loading eccentricity on the normalized critical buckling load for a bi-layer beam-column with delamination that has already developed to a certain stage of $a/L=0.4$ will be examined. It should be mentioned that in some cases there will be no buckling or the critical buckling load cannot be solved if imperfection is accounted for, and this uncertainty will depend on the type or the "value" of the introduced imperfection. For the considered specimen chosen in this study, the eccentric axial load is always applied within the cross section area, and the slenderness ratio for the considered specimen is within a reasonable range, i.e., not too small or too large. As a result, the introduced imperfection resulted from the considered loading eccentricity is small, and the eigenvalue solution of the determinant of the matrix $\mathbf{K}$ always exists, leading to an ever existent critical buckling load of the considered delaminated beam-column. The geometry and material properties of the bi-layer beam-column are the same as the isotropic one examined in Section 4. The variations of the normalized critical buckling load with respect to the loading eccentricity parameter μ for four

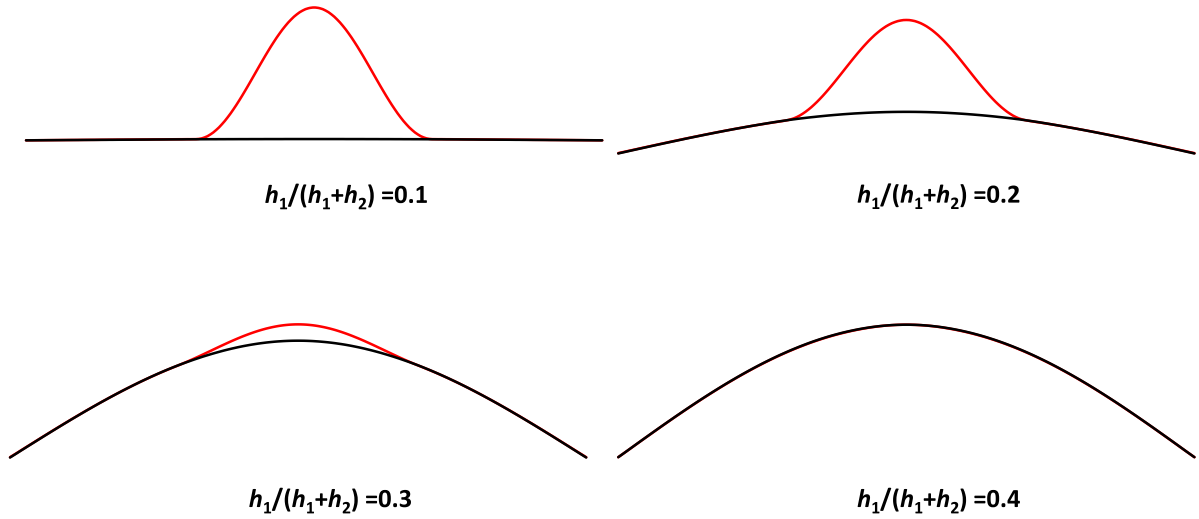

Fig. 9. Buckling mode shapes for bi-layer beam-column with $a/L = 0.4$ and different delaminated thickness ratio.

different delaminated sub-layer ratio cases (i.e., $h_1/(h_1 + h_2) = 0.5$, 0.3, 0.2, and 0.1) are shown in Fig. 10. The loading eccentricity ratio $\mu = e/(h_1 + h_2)$, which is defined in Fig. 2(b), varies from 0 (pure compression) to 0.5 (loaded at the edge point). As expected (see Fig. 10), the buckling strength of the bi-layer beam-column decreases with the increasing of the eccentricity of the applied compression load. However, for the symmetric delamination buckling ($h_1/(h_1 + h_2) = 0.5$) where the buckled mode is primarily controlled by the global behavior (see Fig. 8), as the compression load moves from the mid-plane ($\mu = 0$) to the cross section edge ($\mu = 0.5$) of the beam-column, the effect of loading eccentricity is negligible only with a reduction around 2.7% of critical buckling capacity. However, as the delamination moves outward the surface from the mid-plane, the loading capacity of the beam-column decreases much more observably with the increase of the loading eccentricity. An interesting phenomenon occurs between the delaminated sub-layer ratio $h_1/(h_1 + h_2) = 0.3$ and $h_1/(h_1 + h_2) = 0.2$, where the decreasing trend of the buckling load with the increasing loading eccentricity is convex for the first one (i.e., $h_1/(h_1 + h_2) = 0.3$), which is totally different from the latter one (i.e., $h_1/(h_1 + h_2) = 0.2$) exhibiting a concave decrease. For the moderately thick sub-layers as shown in these two cases, a coexistent global-local buckling mode exists (see Fig. 9). When there is a thin delaminated sub-layer (film) (e.g., $h_1/(h_1 + h_2) = 0.1$) where the local sub-layer delamination buckling controls, the effect of loading eccentricity becomes small but still quite noticeable.

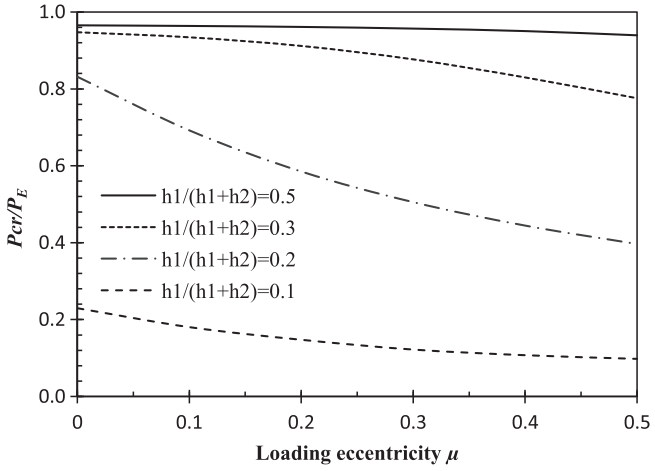

Fig. 10. Effect of loading eccentricity on the normalized critical delamination buckling load in bi-layer beam-column.

5.3. Effect of interface compliance

In the flexible joint model, when the interface is assumed to be infinitely rigid (i.e., $C_n = C_s = 0$), the local delamination tip deformation due to the interface stress diminishes, and the flexible joint model will converge to the semi-rigid joint model. Since both the interface normal and shear stresses contribute to the local delamination tip deformations, the effect of the interface normal compliance C_n resulted from the through-thickness Young's modulus and the shear compliance C_s due to the transverse shear modulus (as shown in Eq. (5)) on the critical buckling load will be separately investigated in this section. The slenderness ratio and thickness of the considered bi-layer beam-column are the same as examined in Section 4, and the delamination length ratio and the delaminated sub-layer thickness ratio are fixed to be, respectively, $a/L = 0.4$, and $h_1/(h_1 + h_2) = 0.2$, in which a combined local-global buckling mode (see Fig. 9) is anticipated. In examining the effect of the interface normal compliance (C_n) on the buckling load, the through-thickness Young's modulus E_{33} varies from $E_{33}/E_{11} = 0.05$ to $E_{33}/E_{11} = 10$, while keeping the longitudinal Young's modulus E_{11}, transverse shear modulus G_{13} and Poisson's ratio υ_{13} the same as the orthotropic material properties studied in Section 4. To study the effect of the interface shear compliance (C_s), the sub-layer transverse shear modulus G_{13} varies from $G_{13}/E_{11} = 0.05$ to $G_{13}/E_{11} = 10$ while keeping the other material properties the same as the orthotropic ones studied in Section 4.

Fig. 11 shows the variation of the normalized critical delamination buckling load with respect to the interface compliances for the bi-layer beam-column under pure compression based on three different joint models as well as the FE model. Overall, a good agreement between the flexible joint model and the FEA is observed. It is obvious from Fig. 11(a) that the solutions predicted by the rigid joint model and semi-rigid joint model are independent of the through-thickness Young's modulus since both of them are based on the one dimensional beam theory. However, as shown in Fig. 11(a), when $\log(E_{33}/E_{11})$ is less than -0.6 (i.e., $E_{33}/E_{11} < 0.25$, which is common in orthotropic composite material), the critical normalized buckling load of the considered bi-layer beam-column decreases rapidly with the decreasing through-thickness Young's modulus, and consequently, the difference between the rigid joint

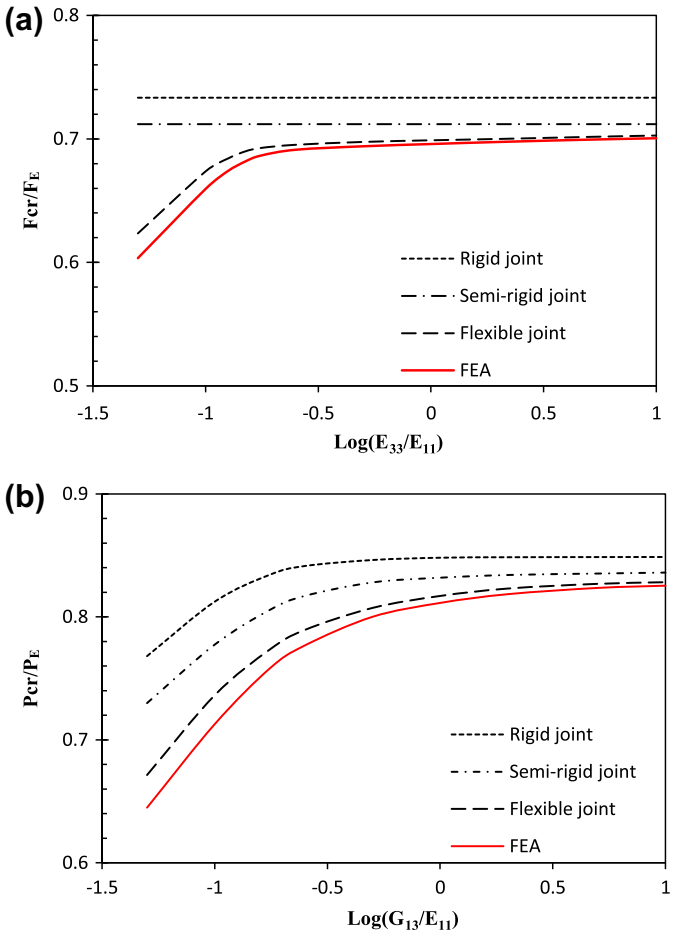

Fig. 11. Effect of interface compliance on the normalized critical delamination buckling load in bi-layer beam-column: (a) interface normal compliance, and (b) interface shear compliance.

model and the flexible joint model becomes much larger. It indicates that both the rigid and semi-rigid joint models significantly overestimate the buckling strength for composite beam-column structures with low through-thickness Young's modulus. On the other hand, the present flexible joint model, to some extent as a pseudo-2D model, is capable of capturing the local delamination tip deformation and thus providing an improved prediction of buckling strength.

The variation of the normalized critical delamination buckling load with respect to the interface shear compliance (C_s) is shown in Fig. 11(b). In this case, the solutions predicted by all the three joint models decrease with the decreasing of the transverse shear modulus. Nevertheless, the differences among three solutions based on three different joint models becomes larger with the decreasing transverse shear modulus, which means that the effect of the interface shear deformation on the buckling behavior is more observable when the interface becomes more shear compliant.

The increasing discrepancies of the critical buckling load among the rigid, semi-rigid, and flexible joint models with the increasing interface compliance coefficients (C_n and C_s) shown in Fig. 11 demonstrate that the local delamination tip deformations are a key factor for accurately evaluating the buckling strength in composite beam-columns, especially for those with material properties of relatively lower through-thickness stiffness and/or transverse shear stiffness. Fig. 11(b) also demonstrates that the transverse shear modulus of the sub-layers plays a significant role to all the three joint models.

6. Conclusions

Based on the flexible joint model (Qiao and Wang, 2004), an improved one-dimensional (1-D) analytical model is developed in this study to analyze the buckling behavior of a delaminated bi-layer composite beam-column. The transverse shear deformation and local delamination tip deformations are taken into consideration by modeling the delaminated sub-layers and intact substrates as individual Timoshenko beams. A deformable interface is introduced to establish the continuity condition at the interface between the intact substrates. As a result, the elastic deformations of the joint, such as differential axial extension, normal peeling and rotations of the two delaminated sub-layers at the delamination tips are fully captured, which completely differs from the conventional rigid joint in most existing studies in the literature where the local delamination tip deformations are fully ignored. Moreover, by accounting for the global deformations of the intact region in the delaminated composite beam-column, the present model is capable of capturing the buckling mode shape transitions from global, to global-local coexistent, and to local buckling for asymmetric delamination buckling as the interface delamination increases. Comparisons among the conventional rigid joint model, semi-rigid joint model, the present flexible joint model, and FEA show that the former two models overestimate the critical buckling load while the solutions predicted by the present model agree well with those evaluated by FEA. On the other hand, it indicates that the local delamination tip deformation plays an important role in accurately evaluating the buckling strength of a delaminated composite beam-column.

Based on the parametric study by the present flexible joint model, the following observations of the effects of loading, geometry and material properties on the buckling behavior of delaminated composite beam-columns are obtained:

(1) When the delamination length ratio is relatively small (e.g., $a/L \leqslant 0.2$), the buckling strength is relatively independent of the through-thickness position of the delamination; while as the delamination moves outward the surface from the mid-plane, the loading capacity of the beam-column will rapidly decrease, and at the same time, gradual transitions of buckling mode shapes from global to combined global-local and finally to sub-layer local delamination buckling take place.

(2) For symmetric delamination buckling ($h_1/(h_1 + h_2) = 0.5$), the effect of loading eccentricity on the buckling load is negligible; as the delamination moves outward the surface from the mid-plane, the loading capacity of the beam-column decreases considerably with the increase of the loading eccentricity.

(3) For orthotropic composite beam-columns with relatively low through-thickness Young's modulus, due to the limit of one dimensional beam theory, the rigid and semi-rigid joint models significantly overestimate the buckling strength when compared with the present model, implying that the present model, to some extent, is a pseudo-2D model for solving composite beam-column buckling problem and capable of capturing the through-thickness effect of beams.

(4) As the interface normal and shear compliances increase, the discrepancies of solutions among the rigid, semi-rigid, and flexible joint models increase, demonstrating that the local delamination tip deformations play a key role for

accurately evaluating the buckling strength of delaminated composite beam-columns, especially for those with material properties of relatively lower through-thickness stiffness and transverse shear stiffness.

In summary, the improved analytical solution based on the flexible joint model presented in this study can be used to better predict the buckling behavior of delaminated composite column and beam-column structures and provides a viable and effective tool when compared to numerical finite element and other high-order beam models.

Appendix A

$$S_{1i}=\frac{1}{A_1}\left(\frac{c_{1i}}{R_1}+\frac{c_{2i}}{R_2}+\frac{c_{3i}}{R_3}\right), i=1,2,3,$$

$$S_{2i}=\frac{1}{D_1}\left(\frac{c_{1i}S_1}{R_1}+\frac{c_{2i}S_2}{R_2}+\frac{c_{3i}S_3}{R_3}\right),\quad i=1,2,3,$$

$$S_{3i}=\left(\frac{S_1}{D_1R_1^2}+\frac{T_1}{B_1R_1}\right)c_{1i}+\left(\frac{S_2}{D_1R_2^2}+\frac{T_2}{B_1R_2}\right)c_{2i}+\left(\frac{S_3}{D_1R_3^2}+\frac{T_3}{B_1R_3}\right)c_{3i},\quad i=1,2,3,$$

$$S_{4i}=-\frac{1}{A_2}\left(\frac{c_{1i}}{R_1}+\frac{c_{2i}}{R_2}+\frac{c_{3i}}{R_3}\right),\quad i=1,2,3,$$

$$S_{5i}=-\frac{1}{D_2}\left(\frac{c_{1i}S_1'}{R_1}+\frac{c_{2i}S_2'}{R_2}+\frac{c_{3i}S_3'}{R_3}\right),\quad i=1,2,3,$$

$$S_{6i}=-\left(\frac{S_1'}{D_2R_1^2}+\frac{T_1}{B_2R_1}\right)c_{1i}-\left(\frac{S_2'}{D_2R_2^2}+\frac{T_2}{B_2R_2}\right)c_{1i}-\left(\frac{S_3'}{D_2R_3^2}+\frac{T_3}{B_2R_3}\right)c_{1i},\quad i=1,2,3,$$

and

$$S_i=\frac{\eta}{\xi}-\frac{R_i^2}{bK_s\xi},\ T_i=-\left(S_i+\frac{h_1}{2}\right)R_i,\ S_i'=S_i+\frac{h_1+h_2}{2},\quad i=1,2,3,$$

$$\begin{pmatrix}c_1\\c_2\\c_3\end{pmatrix}=\begin{pmatrix}c_{11}&c_{12}&c_{13}\\c_{21}&c_{22}&c_{23}\\c_{31}&c_{32}&c_{33}\end{pmatrix}\begin{pmatrix}N\\M\\Q\end{pmatrix}=\frac{1}{Y}\begin{pmatrix}-S_2T_3+S_3T_2&-T_2+T_3&S_2-S_3\\S_1T_3-S_3T_1&T_1-T_3&-S_1+S_3\\-S_1T_2+S_2T_1&-T_1+T_2&S_1-S_2\end{pmatrix}\begin{pmatrix}N\\M\\Q,\end{pmatrix}$$

$$Y=(S_2-S_3)T_1-(S_1-S_3)T_2+(S_1-S_2)T_3.$$

References

Adam, C., Heuer, R., Jeschko, A., 1997. Flexural vibrations of elastic composite beams with interlayer slip. Acta Mechanica 125, 17–30.

Andrews, M.G., Massabo, R., 2007. The effects of shear and near tip deformations on energy release rate and mode mixity of edge-cracked orthotropic layers. Engineering Fracture Mechanics 74, 2700–2720.

Bažant, Z.P., Cedolin, L., 1991. Stability of Structures: Elastic, Inelastic, Fracture and Damage Theories. Oxford University Press, New York.

Battini, J.-M., Nguyen, Q.-H., Hjiaj, M., 2009. Non-linear finite element analysis of composite beams with interlayer slips. Computers and Structures 87, 904–912.

Cas, B., Saje, M., Planinc, I., 2007. Buckling of layered wood columns. Advances in Engineering Software 38, 586–597.

Chai, H., 1982. The Growth of Impact Damage in Compressively Loaded Laminates. Dissertation (Ph.D.), California Institute of Technology, Pasadena, CA.

Chai, H., Babcock, C.D., Knauss, W.G., 1981. One dimensional modelling of failure in laminated plates by delamination buckling. International Journal of Solids and Structures 17, 1069–1083.

Chen, F., Qiao, P., 2010. Electromechanical behavior of interface deformable piezoelectric bilayer beams. Journal of Engineering Mechanics 136, 413–428.

Chen, H.P., 1991. Shear deformation theory for compressive delamination buckling and growth. AIAA Journal 29, 813–819.

Chen, H.P., 1993. Transverse shear effects on buckling and postbuckling of laminated and delaminated plates. AIAA Journal 31, 163–169.

Girhammar, U.A., Pan, D.H., 2007. Exact static analysis of partially composite beams and beam-columns. International Journal of Mechanical Sciences 49, 239–255.

Kardomateas, G.A., Shmueser, D.W., 1998. Buckling and postbuckling of delaminated composites under compressive loads including transverse shear effects. AIAA Journal 26, 337–343.

Kryzanowski, A., Saje, M., Planinc, I., Zupan, D., 2008. Analytical solution for buckling of asymmetrically delaminated Reissner's elastic columns including transverse shear. International Journal of Solids and Structures 45, 1051–1070.

Kryzanowski, A., Schnabl, S., Turk, G., Planinc, I., 2009. Exact slip-buckling analysis of two-layer composite columns. International Journal of Solids and Structures 46, 2929–2938.

Moradi, S., Taheri, F., 1999. Delamination buckling analysis of general laminated composite beams by differential quadrature method. Composites Part B: Engineering 30, 503–511.

Ovesy, H.R., Kharazi, M., 2011. Stability analysis of composite plates with through-the-width delamination. Journal of Engineering Mechanics 137, 87–100.

MSRao, P., Shu, D., 2004. Buckling analysis of two-layer beams with an asymmetric delamination. Engineering Structures 26, 651–658.

Planinc, I., Schnabl, S., Saje, M., Lopatic, J., Cas, B., 2008. Numerical and experimental analysis of timber composite beams with interlayer slip. Engineering Structures 30, 2959–2969.

Qiao, P., Chen, F., 2008. An improved adhesively bonded bi-material beam model for plated beams. Engineering Structures 30, 1949–1957.

Qiao, P., Chen, F., 2009. Interface crack between two interface deformable piezoelectric layers. International Journal of Fracture 156, 185–201.

Qiao, P., Chen, F., 2011. On the compliance and energy release rate of generically-unified beam-type fracture specimens. Journal of Composite Materials 45, 65–101.

Qiao, P., Shan, L., Chen, F., Wang, J., 2010. Local delamination buckling of laminated composite beams using novel joint deformation models. Journal of Engineering Mechanics 136, 541–550.

Qiao, P., Wang, J., 2004. Mechanics and fracture of crack tip deformable bi-material interface. International Journal of Solids and Structures 41, 7423–7444.

Schnabl, S., Planinc, I., 2010. The influence of boundary conditions and axial deformability on buckling behavior of two-layer composite columns with interlayer slip. Engineering Structures 32, 3103–3111.

Schnabl, S., Planinc, I., 2011. The effect of transverse shear deformation on the buckling of two-layer composite columns with interlayer slip. International Journal of Non-Linear Mechanics 46, 543–553.

Schnabl, S., Saje, M., Turk, G., Planinc, I., 2007. Analytical solution of two-layer beam taking into account interlayer slip and shear deformation. Journal of Structural Engineering 133, 886–894.

Short, G.J., Guild, F.J., Pavier, M.J., 2001. The effect of delamination geometry on the compressive failure of composite laminates. Composites Science and Technology 61, 2075–2086.

Shu, D., MSRao, P., 2004. Buckling analysis of bimaterial beams with single asymmetric delamination. Composite Structures 64, 501–509.

Wang, J., Qiao, P., 2004a. Novel beam analysis of end notched flexure specimen for mode-II fracture. Engineering Fracture Mechanics 71, 219–231.

Wang, J., Qiao, P., 2004b. Interface crack between two shear deformable elastic layers. Journal of the Mechanics and Physics of Solids 52, 891–905.

Wang, J., Zhang, C., 2009. Energy release rate and phase angle of delamination in sandwich beams and symmetric adhesively bonded joints. International Journal of Solids and Structures 46, 4409–4418.

Yin, W.L., 1988. The effects of laminated structure on delamination buckling and growth. Journal of Composite Materials 22, 502–517.

Yin, W.L., Sallam, S.N., Simitses, G.J., 1986. Ultimate axial load-capacity of a delaminated beam-plate. AIAA Journal 24, 123–128.

Yin, W.-L., 1998. Thermomechanical buckling of delaminated composite laminates. International Journal of Solids and Structures 35, 2639–2653.